Monthly Notices
of the
ROYAL ASTRONOMICAL SOCIETY

MNRAS **468,** L63–L67 (2017)
Advance Access publication 2017 February 11

doi:10.1093/mnrasl/slx027

Galactic rotation in *Gaia* DR1

Jo Bovy[1,2]★†

[1]*Department of Astronomy and Astrophysics, University of Toronto, 50 St. George Street, Toronto, ON M5S 3H4, Canada*
[2]*Center for Computational Astrophysics, Flatiron Institute, 162 5th Ave, New York, NY 10010, USA*

Accepted 2017 February 8. Received 2017 February 7; in original form 2016 December 23

ABSTRACT

The spatial variations of the velocity field of local stars provide direct evidence of Galactic differential rotation. The local divergence, shear and vorticity of the velocity field – the traditional Oort constants – can be measured based purely on astrometric measurements and in particular depend linearly on proper motion and parallax. I use data for 304 267 main-sequence stars from the *Gaia* DR1 Tycho-*Gaia* Astrometric Solution to perform a local, precise measurement of the Oort constants at a typical heliocentric distance of 230 pc. The pattern of proper motions for these stars clearly displays the expected effects from differential rotation. I measure the Oort constants to be: $A = 15.3 \pm 0.4\,\mathrm{km\,s^{-1}\,kpc^{-1}}$, $B = -11.9 \pm 0.4\,\mathrm{km\,s^{-1}\,kpc^{-1}}$, $C = -3.2 \pm 0.4\,\mathrm{km\,s^{-1}\,kpc^{-1}}$ and $K = -3.3 \pm 0.6\,\mathrm{km\,s^{-1}\,kpc^{-1}}$, with no colour trend over a wide range of stellar populations. These first confident measurements of C and K clearly demonstrate the importance of non-axisymmetry for the velocity field of local stars and they provide strong constraints on non-axisymmetric models of the Milky Way.

Key words: stars: kinematics and dynamics – Galaxy: disc – Galaxy: fundamental parameters – Galaxy: kinematics and dynamics – solar neighbourhood.

1 INTRODUCTION

Determining the rotation of the Milky Way's disc is difficult, because our vantage point is corotating with the local stars. As first pointed out by Oort (1927) and generalized by Ogrodnikoff (1932), the local rotational frequency and the local change in the circular velocity can be determined from the pattern of line-of-sight velocities and proper motions of nearby stars as a function of Galactic longitude l. Expanding the Milky Way's in-plane velocity field to first order in heliocentric distance in an axisymmetric velocity field, the azimuthal shear and vorticity contribute terms proportional to $\cos 2l$, $\sin 2l$ and a constant to the mean proper-motion and line-of-sight velocity, which can be distinguished from the $\cos l$ and $\sin l$ pattern due to the Sun's peculiar motion with respect to nearby stars. Going beyond the axisymmetric approximation, the radial shear and divergence contribute similar $\cos 2l$, $\sin 2l$ and constant terms. The four first-order terms (azimuthal and radial shears, vorticity and divergence) are known as the Oort constants. Measurements of these constants provided the first strong evidence that the Milky Way is rotating differentially with a close-to-flat rotation curve (Oort 1927).

The current best measurements of the Oort constants use Cepheids to investigate the velocity field on large scales (>1 kpc) with a kinematically cold stellar tracer population (e.g. Feast & Whitelock 1997; Metzger, Caldwell & Schechter 1998). Because the relative contribution to the velocity pattern from the Sun's peculiar motion to that from Galactic rotation diminishes as the inverse of the distance, the intrinsic velocity field can be more easily determined from such large-scale observations. However, higher order contributions to the velocity field become important at large distances and the derived values for the Oort constants may not reflect their local value. Local measurements require large stellar samples with good velocity measurements. Olling & Dehnen (2003) attempted a local measurement using proper motions from the Tycho-2 catalogue (Høg et al. 2000) that was complicated by the unknown distance distribution at different l, which produces spurious terms in the velocity pattern that are difficult to distinguish from the effects of Galactic rotation.

The *Gaia* mission (Gaia Collaboration et al. 2016a) has recently released its first set of data, including parallaxes and proper motions for about 2 million Tycho-2 stars in the Tycho–*Gaia* Astrometric Solution (TGAS; Michalik, Lindegren & Hobbs 2015; Gaia Collaboration et al. 2016b; Lindegren et al. 2016). This large set of astrometric measurements allows the first truly local precise measurement of the Oort constants. I discuss the definition and interpretation of the Oort constants in Section 2. I describe the data used in this Letter in detail in Section 3 and the measurement of the Oort constants in Section 4. I discuss the results in Section 5.

2 DEFINITIONS

The four Oort constants A, B, C and K are a representation of the four first-order expansion coefficients of the two-dimensional, in-plane mean velocity field of a stellar population in a Taylor series expansion of the mean velocity field with respect to distance from

★ E-mail: bovy@astro.utoronto.ca
† Alfred P. Sloan Fellow.

the Sun. For a given stellar population, in Galactocentric cylindrical coordinates (R, ϕ) with the Sun at $(R_0, 0)$ they are given by

$$
\begin{aligned}
2A &= \bar{v}_\phi/R_0 - \bar{v}_{\phi,R} - \bar{v}_{R,\phi}/R_0\,,\\
2B &= -\bar{v}_\phi/R_0 - \bar{v}_{\phi,R} + \bar{v}_{R,\phi}/R_0\,,\\
2C &= -\bar{v}_R/R_0 + \bar{v}_{R,R} - \bar{v}_{\phi,\phi}/R_0\,,\\
2K &= \bar{v}_R/R_0 + \bar{v}_{R,R} + \bar{v}_{\phi,\phi}/R_0\,,
\end{aligned}
$$

where subscripts , R and , ϕ denote derivatives with respect to R and ϕ, respectively, and these derivatives are evaluated at the Sun's position. In these expressions, $(\bar{v}_\phi, \bar{v}_R)$ are the mean rotational and radial velocities, respectively, of the stellar population. The proper motion (μ_l, μ_b) of the stellar population can be expressed in terms of these constants as

$$
\begin{aligned}
\mu_l(l, b, \varpi) = &(A\,\cos 2l - C\,\sin 2l + B)\,\cos b\\
&+ \varpi\,(u_0\,\sin l - v_0\,\cos l)\,,
\end{aligned}
\tag{1}
$$

and

$$
\begin{aligned}
\mu_b(l, b, \varpi) = &-(A\,\sin 2l + C\,\cos 2l + K)\,\sin b\,\cos b\\
&+ \varpi\,[(u_0\,\cos l + v_0\,\sin l)\,\sin b - w_0\,\cos b]\,,
\end{aligned}
\tag{2}
$$

where (u_0, v_0, w_0) is the Sun's motion with respect to the stellar population and ϖ is the inverse distance to the stars. See Olling & Dehnen (2003) for an elegant derivation of these relations.

In the discussion above, the term 'Oort constants' is a misnomer because (i) they vary for different stellar populations, and (ii) even for a given stellar population they are not constant in time. Historically, the Oort constants have been defined based on a population of stars on (hypothetical) closed orbits, for which a measurement of the Oort constants provides direct constraints on the gravitational potential (which directly sets the properties of closed orbits). Under the further assumption that the Galaxy is axisymmetric, $C = K = 0$ and $\bar{v}_\phi = V_c = R\,\partial\Phi/\partial R$, the circular velocity for the axisymmetric potential Φ, and A and B then provide direct measurements of the angular rotation frequency $\Omega_0 = V_c/R_0$ at the Sun and the local slope of the rotation curve $\mathrm{d}V_c/\mathrm{d}R$.

The real Galaxy, however, is not this simple. First, all stars have attained a random component to their orbital energy that causes their orbits to be eccentric and non-closed, even in an axisymmetric potential. Thus, their mean velocity field is not related in a simple manner to the gravitational potential. Secondly, non-axisymmetric or time-dependent perturbations to the potential complicate the orbits of even the coldest stellar populations and they typically no longer close. The first effect can in principle be accounted for in a relatively straightforward manner for well-mixed stellar populations in an axisymmetric potential (Bovy 2015), but in the likely situation that the second effect is relevant, no precise, general relation between the Oort constants and the potential of the Milky Way exist. In this case, the measured values of the 'Oort constants' merely provide a strong constraint on the potential.

3 DATA

I employ parallaxes and proper motions from the *Gaia* DR1 TGAS catalogue, which have typical uncertainties of 0.3 mas and 1 mas yr^{-1}, respectively. I consider only the 450 278 TGAS sources with relative parallax uncertainties less than 10 per cent and with inverse parallaxes less than 500 pc to select a local sample. In order to separate stellar populations into kinematically colder and warmer populations, I use matched photometry from the AAVSO Photometric All-Sky Survey (APASS; Henden et al. 2012) for the 355 753 stars with APASS photometry to construct the $(B - V, M_V)$ colour–magnitude diagram displayed in Fig. 1. I select main-sequence stars using the cuts shown in this figure – simply chosen by hand to encompass the main sequence with minimal contamination, which creates a sample of 315 946 stars.

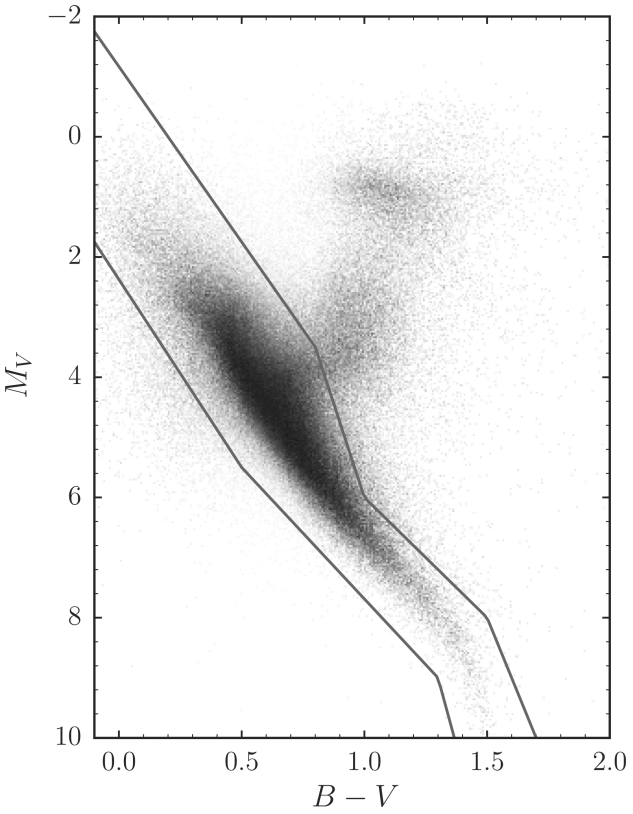

Figure 1. Color–magnitude diagram for 355 753 TGAS stars with relative parallax uncertainties less than 10 per cent within 500 pc that have (B, V) photometry from APASS. The grey curves indicate the cuts that are employed to select the 315 946 main-sequence stars that are used in this Letter.

For this sample, I convert the proper motions in equatorial coordinates to Galactic coordinates and propagate the proper-motion uncertainty covariance matrix through this transformation as well. Proper motions in mas yr^{-1} are converted to units of km s^{-1} kpc^{-1} by multiplying them by 4.740 47. In what follows, I ignore the correlations between the measurements of the parallax and the Galactic proper motions, because the scatter in the proper motions is dominated by intrinsic scatter (the intrinsic scatter is $\approx$150 km s^{-1} kpc^{-1} due to the small distance range of the sample versus typical measurement uncertainties $\lesssim$5 km s^{-1} kpc^{-1}). Decorrelating the parallax and proper motion errors by adding random, uncorrelated noise that is four times larger than the formal uncertainties gives changes in the inferred Oort constants below $\lesssim$0.2 km s^{-1} kpc^{-1}, confirming that the parallax–proper-motion correlation is a subdominant source of uncertainty.

4 MEASUREMENT

It is clear from the expressions in equations (1) and (2) that the Oort constants can be measured purely based on astrometric quantities $(l, b, \varpi, \mu_l, \mu_b)$. The astrometric quantities (ϖ, μ_l, μ_b) appear in a linear fashion and are therefore well behaved. Specifically, it is unnecessary to invert the parallax to obtain a distance for the

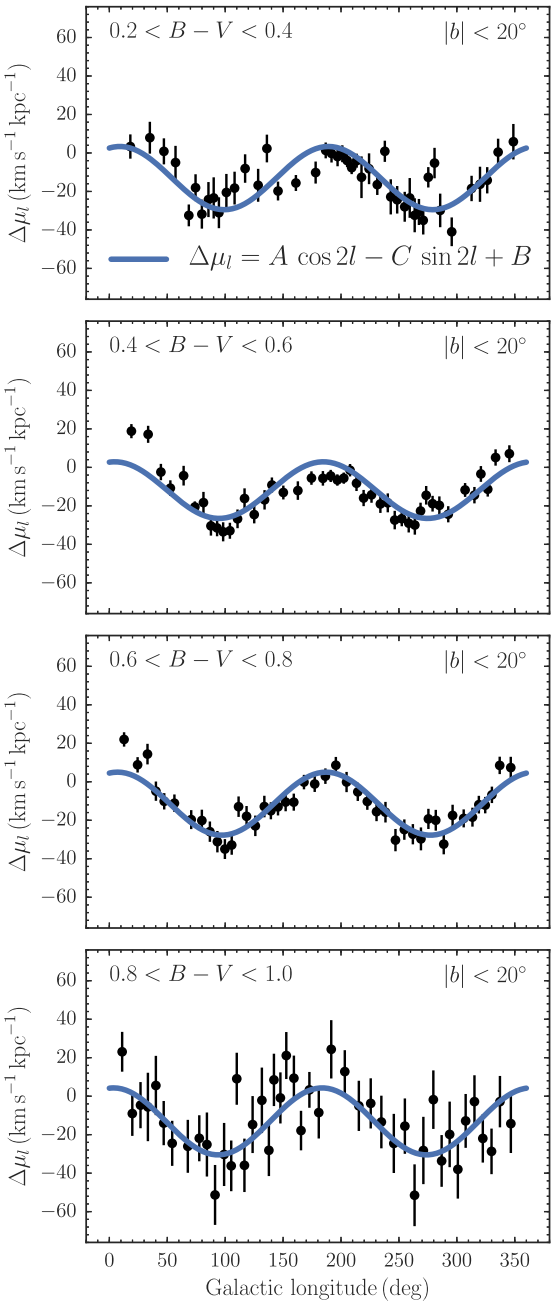

Figure 2. Comparison between the observed mean proper motion in Galactic longitude corrected for the solar motion (see equation 3) as a function of l and the best-fitting model for the four main colour bins used in the analysis. The data clearly display the expected signatures due to the differential rotation of the Galactic disc. The agreement between the model and the data is good.

measurement of the Oort constants. I model the observed individual proper motions using the model in equations (1) and (2), adding intrinsic Gaussian scatter to account for the non-zero velocity dispersion. The free parameters are therefore (A, B, C, K, u_0, v_0, w_0) and two free parameters (σ_{μ_l}, σ_{μ_b}) describing the Gaussian scatter in (μ_l, μ_b).[1]

[1] For simplicity, the scatter is assumed to be independent of (l, b, ϖ). This assumption is incorrect in detail, because the velocity ellipsoid in the solar neighbourhood is triaxial (e.g. Dehnen & Binney 1998). However, it does not negatively impact the results obtained here, because it will cause only the inferred scatter to be too large at some (l, b, ϖ). This does not bias the best-fitting value of the parameters (A, B, C, K, u_0, v_0, w_0) describing the mean trend of $\mu_l(l)$ and $\mu_b(l)$ given in equations (1) and (2), but it will slightly overestimate the uncertainties in these values.

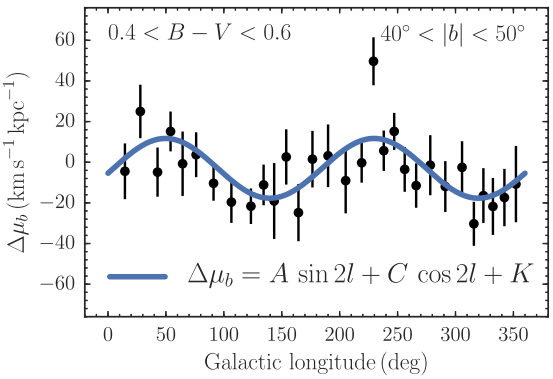

Figure 3. Same as Fig. 2, but for the proper motion in Galactic latitude for a single colour bin with many stars at the intermediate latitudes where Galactic rotation is clearest. The proper motion is corrected for the solar motion (see equation 4). The data display the expected sin 2l behaviour due to differential rotation and the non-zero mean offset shows that the local divergence is non-zero due to non-axisymmetric motions.

I fit the data (μ_l^i, μ_b^i) with associated uncertainties ($s_{\mu_l}^i$, $s_{\mu_b}^i$) sliced in 0.2 mag bins in $B-V$ using the log likelihood:

$$\ln\mathcal{L} = -\frac{1}{2}\sum_i \left(\frac{[\mu_l^i - \mu_l(l_i, b_i, \varpi_i)]^2}{\sigma_{\mu_l}^2 + (s_{\mu_l}^i)^2} + \ln[\sigma_{\mu_l}^2 + (s_{\mu_l}^i)^2] + \frac{[\mu_b^i - \mu_b(l_i, b_i, \varpi_i)]^2}{\sigma_{\mu_b}^2 + (s_{\mu_b}^i)^2} + \ln\left[\sigma_{\mu_b}^2 + (s_{\mu_b}^i)^2\right] \right).$$

The parameters A, C, u_0 and v_0 are constrained by both components of the proper motions; fitting them separately to μ_l and μ_b gives consistent results for all four of these. I determine the uncertainty in the best-fitting parameters using Markov chain Monte Carlo (MCMC) with flat priors on all parameters. Note that all parameters except the scatter terms are linear parameters whose probability distribution at fixed scatter could be obtained analytically, but because we need to fit for the non-linear scatter parameters I do not make use of this simplification.

The best-fitting model to four colour bins is compared to the μ_l data in Fig. 2. Because the solar motion is the dominant effect on $\mu_l(l)$ that obscures the Galactic rotation contribution, the observed proper motions in this figure have been corrected for the solar motion (u_0, V_0) using the best-fitting parameters as follows:

$$\Delta\mu_l(l) = (\mu_l - \varpi\,[u_0\,\sin l + v_0\,\cos l])\,/\,\cos b\,, \qquad (3)$$

such that the mean $\Delta\mu_l(l) = A\cos 2l - C\sin 2l + B$. The data are binned to display the mean $\Delta\mu_l(l)$ because of the large scatter of individual data points. On account of the $1/\cos b$ correction, in Fig. 2, I only show stars with $|b| < 20°$ that display the trend most clearly, even though stars at all b are used in the fit.

The proper motion in Galactic latitude is much more tenuously related to the parameters of Galactic rotation on account of the $\sin b\cos b$ factor in equation (2). Therefore, I compare only the data and the model in Fig. 3 for the single $B-V$

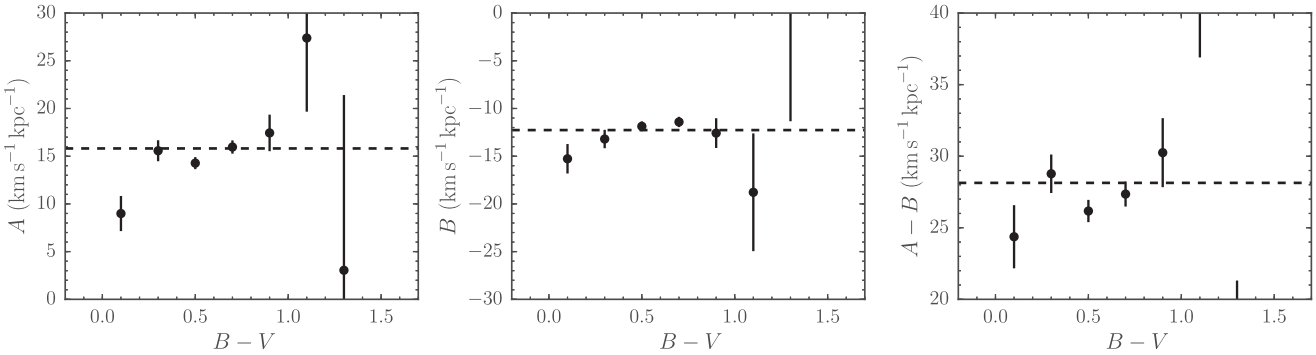

Figure 4. Measurements of A, B and $A-B$ from the TGAS sample for different colour bins. The measured values from different colour bins agree well, except for the bluest, youngest stars, which may be affected by streaming motions at birth. The dashed line in each panel indicates the combined measurement from the four colour bins blueward of $B-V=1$ (except for the bluest bin).

bin that contains enough stars at intermediate b to allow for a straightforward data–model comparison. Similar to Fig. 2, the proper motion in Fig. 3 is corrected for the solar motion as follows:

$$\Delta\mu_b(l) = -(\mu_b - \varpi\,[(u_0\cos l + v_0\sin l)\sin b - w_0\cos b])/(\sin b\cos b)\,, \quad (4)$$

such that the mean $\Delta\mu_b(l) = A\sin 2l + C\cos 2l + K$. The data are again binned to display the mean trend and I restrict the sample to stars with $40^\circ < |b| < 50^\circ$, even though stars at all b are used in the fit.

Overall the data display good agreement with the simple first-order velocity model in both $\mu_l(l)$ and $\mu_b(l)$. The posterior probability distribution for the Oort and solar-motion parameters displays no correlations among any of the parameters, as expected from the full and close to uniform coverage in l of the stars in the TGAS sample.

Fig. 4 shows the measurements of A, B and $A-B$, which is equal to the rotational frequency Ω_0 if the Galaxy were axisymmetric, as a function of $B-V$. The different colour bins display excellent agreement with each other, except for the very bluest stars, which are likely affected by residual streaming motions from birth. That A and B do not strongly depend on colour (and, thus, on velocity dispersion) is expected in the limit of well-mixed, solar-neighbourhood populations in an axisymmetric Galaxy, for which A and B should be constant to within $\lesssim 1\,\mathrm{km\,s^{-1}\,kpc^{-1}}$ (Bovy 2015). I combine the four bins blueward of $B-V=1$ (except for the bluest bin), which contain the majority of the stars in the sample (304 267 out of 315 946) to obtain a single value of each Oort constant. The combined measurements are $A = 15.3 \pm 0.4\,\mathrm{km\,s^{-1}\,kpc^{-1}}$, $B = -11.9 \pm 0.4\,\mathrm{km\,s^{-1}\,kpc^{-1}}$ as well as $A - B = 27.1 \pm 0.5\,\mathrm{km\,s^{-1}\,kpc^{-1}}$ and $-(A+B) = -3.4 \pm 0.6\,\mathrm{km\,s^{-1}\,kpc^{-1}}$.

The measurements of C and K are displayed in Fig. 5. Like for A and B, the measurements of C and K in different colour bins agree with each other. The measurements are $C = -3.2 \pm 0.4\,\mathrm{km\,s^{-1}\,kpc^{-1}}$ and $K = -3.3 \pm 0.6\,\mathrm{km\,s^{-1}\,kpc^{-1}}$. The reason that the uncertainty in K is larger than that in the other parameters is that it can only be determined from the behaviour of $\mu_b(l)$. I also find that $K + C = \frac{\partial \bar{v}_R}{\partial R}|_{R_0} = -6.6 \pm 0.7\,\mathrm{km\,s^{-1}\,kpc^{-1}}$. The best-fitting C and K are therefore both significantly non-zero, indicating that the local kinematics is non-axisymmetric. There is no trend in colour for either C or K, in disagreement with the previous measurements from Olling & Dehnen (2003).

5 DISCUSSION AND CONCLUSION

I have determined the Oort constants using astrometric measurements for 304 267 local (typical distance of 230 pc) main-sequence stars from the *Gaia* DR1 TGAS catalogue:

$$A = \quad 15.3 \pm 0.4\,\mathrm{km\,s^{-1}\,kpc^{-1}}\,, \quad (5)$$

$$B = -11.9 \pm 0.4\,\mathrm{km\,s^{-1}\,kpc^{-1}}\,, \quad (6)$$

$$C = -3.2 \pm 0.4\,\mathrm{km\,s^{-1}\,kpc^{-1}}\,, \quad (7)$$

$$K = -3.3 \pm 0.6\,\mathrm{km\,s^{-1}\,kpc^{-1}}. \quad (8)$$

These measurements for A and B are in good agreement with those obtained from modelling the *Hipparcos* proper motions of Cepheids: $A = 14.82 \pm 0.84\,\mathrm{km\,s^{-1}\,kpc^{-1}}$ and $B = -12.37 \pm 0.64\,\mathrm{km\,s^{-1}\,kpc^{-1}}$ (Feast & Whitelock 1997). The measurement of A is also in good agreement with that measured from the line-of-sight velocities of Cepheids: $A = 15.5 \pm 0.4 \pm 1.2\,(\mathrm{syst.})\,\mathrm{km\,s^{-1}\,kpc^{-1}}$ (Metzger et al. 1998). Unlike these measurements, the current measurements are based on a sample of stars within a few 100 pc from the Sun and thus truly measure the local velocity field.

The TGAS data also allow a confident measurement of C and K. There are only a few previous measurements of these constants. Olling & Dehnen (2003) measured C from the Tycho-2 proper motions, correcting for the influence of the unknown distance distribution, and found $C = -10 \pm 2\,\mathrm{km\,s^{-1}\,kpc^{-1}}$ and that C is more negative for older, kinematically warmer populations. We find that $C = -3.2 \pm 0.4\,\mathrm{km\,s^{-1}\,kpc^{-1}}$ with no dependence on the colour or velocity dispersion of the stellar population. Previous measurements of K using young stars find that it is negative with typical values in the range $-3\,\mathrm{km\,s^{-1}\,kpc^{-1}}$ to $-1\,\mathrm{km\,s^{-1}\,kpc^{-1}}$ (Comeron, Torra & Gomez 1994; Torra, Fernández & Figueras 2000) in agreement with the present measurement. The measurement of $K + C = \frac{\partial \bar{v}_R}{\partial R}|_{R_0} = -6.6 \pm 0.7\,\mathrm{km\,s^{-1}\,kpc^{-1}}$ is in good agreement with the measurement of the local mean-radial-velocity gradient from Siebert et al. (2011).

That C and K are both non-zero for all colour-selected stellar populations provides strong evidence that the local velocity field is shaped by non-axisymmetric forces. The localized nature of the measurements using the TGAS sample makes these measurements

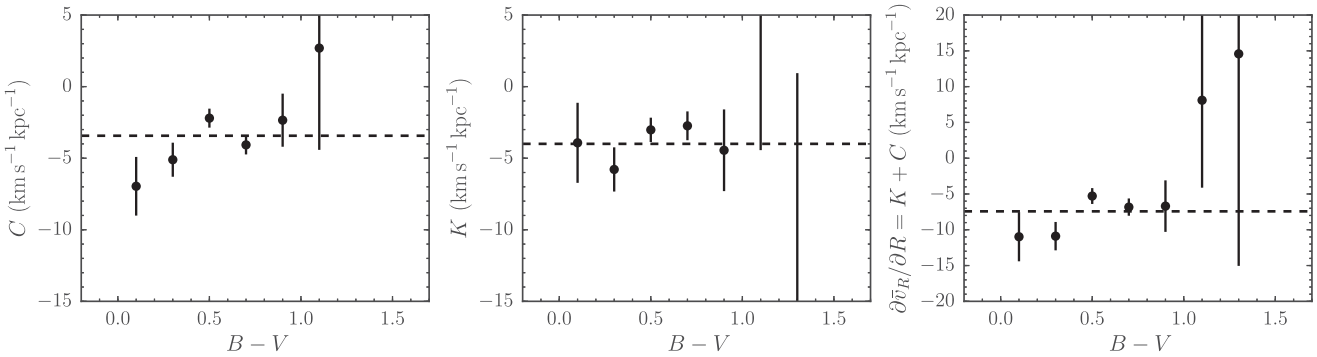

Figure 5. Measurements of C, K and $K + C$ from the TGAS sample for different colour bins. The values derived from all of the different colour bins show good agreement, with no hint of a trend with colour in any of the measurements. The dashed line in each panel indicates the combined measurement from the four colour bins blueward of $B - V = 1$ (except for the bluest bin).

straightforward constraints on any large-scale non-axisymmetric model such as the bar or spiral arms, in which the Oort constants may simply be evaluated at the position of the Sun and compared to these measurements. For example, for no plausible model with a triaxial bulge or halo in which closed orbits are elliptical do C and K have the same sign (Kuijken & Tremaine 1994; Bovy 2015), such that this model on its own is inconsistent with the current measurements. For an axisymmetric disc plus bar model with the bar's outer Lindblad resonance near the Sun – which can explain the Hercules moving group in the local velocity distribution (Dehnen 2000) and the power spectrum of velocity fluctuations in the disc (Bovy et al. 2015) – C and K are both negative with $C \approx K \approx -2\,\mathrm{km\,s^{-1}\,kpc^{-1}}$ (computed using GALPY; Bovy 2015); although kinematically colder populations in this model respond differently to the bar perturbation and give different C (Minchev, Nordhaus & Quillen 2007), which is not observed in the TGAS data. More sophisticated modelling is required to better interpret the measurements of the Oort constants presented here.

That $|C| \approx |K| \approx 0.2 \times |A|$ means that non-circular streaming motions in the solar neighbourhood are important and that A and B cannot be directly related to the Milky Way's circular velocity and its slope at the Sun, as is commonly assumed (see Section 2). A simple estimate of the difference between the value of the circular velocity derived from local measurements of A and B (which is $[A - B]\,R_0 \approx 220\,\mathrm{km\,s^{-1}}$ using the measured A and B and $R_0 \approx 8\,\mathrm{kpc}$) and the global, azimuthally averaged value is $(|C| + |K|)/(|A| + |B|) \approx 20$ per cent or $\approx 40\,\mathrm{km\,s^{-1}}$ for a circular velocity $\approx 220\,\mathrm{km\,s^{-1}}$. This result more generally applies to determinations of the circular velocity from the local kinematics of stars or gas, which are affected by similar streaming motions.

ACKNOWLEDGEMENTS

I thank Dustin Lang for providing the TGAS-matched APASS data, the 2016 NYC *Gaia* Sprint participants for stimulating discussions, and the anonymous referee for a helpful report. I also thank Maarten Breddels for finding and fixing a bug in Figs 2 and 3. JB received support from the Natural Sciences and Engineering Research Council of Canada. JB also received partial support from an Alfred P. Sloan Fellowship and from the Simons Foundation. The MCMC analyses in this work were run using EMCEE (Foreman-Mackey et al. 2013).

This project was developed in part at the 2016 NYC *Gaia* Sprint, hosted by the Center for Computational Astrophysics at the Simons Foundation in New York City.

This work has made use of data from the European Space Agency (ESA) mission *Gaia* (http://www.cosmos.esa.int/gaia), processed by the *Gaia* Data Processing and Analysis Consortium (DPAC, http://www.cosmos.esa.int/web/gaia/dpac/consortium). Funding for the DPAC has been provided by national institutions, in particular the institutions participating in the *Gaia* Multilateral Agreement. This research was made possible through the use of the APASS, funded by the Robert Martin Ayers Sciences Fund.

REFERENCES

Bovy J., 2015, ApJS, 216, 29
Bovy J., Bird J. C., García Pérez A. E., Majewski S. R., Nidever D. L., Zasowski G., 2015, ApJ, 800, 83
Comeron F., Torra J., Gomez A. E., 1994, A&A, 286, 789
Dehnen W., 2000, AJ, 119, 800
Dehnen W., Binney J. J., 1998, MNRAS, 298, 387
Feast M., Whitelock P., 1997, MNRAS, 291, 683
Foreman-Mackey D., Hogg D. W., Lang D., Goodman J., 2013, PASP, 125, 306
Gaia Collaboration et al., 2016a, A&A, 595, A1
Gaia Collaboration et al., 2016b, A&A, 595, A2
Høg E. et al., 2000, A&A, 355, 27
Henden A. A., Levine S. E., Terrell D., Smith T. C., Welch D., 2012, J. Am. Assoc. Var. Star Obs., 40, 430
Kuijken K., Tremaine S., 1994, ApJ, 421, 178
Lindegren L. et al., 2016, A&A, 595, A4
Metzger M. R., Caldwell J. A. R., Schechter P. L., 1998, AJ, 115, 635
Michalik D., Lindegren L., Hobbs D., 2015, A&A, 574, 115
Minchev I., Nordhaus J., Quillen A. C., 2007, ApJ, 664, L31
Ogrodnikoff K., 1932, Z. Astrophysik, 4, 190
Olling R. P., Dehnen W., 2003, ApJ, 599, 275
Oort J. H., 1927, Bull. Astron. Inst. Neth., 3, 275
Siebert A. et al., 2011, MNRAS, 412, 2026
Torra J., Fernández D., Figueras F., 2000, A&A, 359, 82

This paper has been typeset from a TEX/LATEX file prepared by the author.